Fundamentals of Vibration Analysis and Vibroacoustics
Module 1 - Fundamentals of Vibration Analysis
Assignment 3 - Modal parameter identification

Bombaci Nicola 10677942
Fantin Jacopo 10591775
Intagliata Emanuele 10544878

May 2020

In this problem, we're given a small set of measurements we have to extract information from. The virtual experiment consists in a hammer hitting impulsively a structure in one point, and measuring the displacements in four different positions, one of which is where the force is applied (the first one). The initial data are wherefore the time axis t used to represent the sampled measurements and the force, the impulse-like input force $F(t)$, and the four measurements:

$$t \ , \ F(t) \ , \ x_1(t) \ , \ x_2(t) \ , \ x_3(t) \ , \ x_4(t)$$

1 Experimental FRFs

The Frequency Response Functions linking the displacement of the four points to the external force can be retrieved computing the ratio between the Discrete Fourier Transform (DFT) of the former and of the latter. We used the Matlab function `fft` to find the DFT of the function input, here denoted with $\mathcal{F}[\cdot]$, through an optimized Fast Fourier Transform algorithm.

$$H_k^{\text{exp}}(f) = \frac{\mathcal{F}[x_k(t)]}{\mathcal{F}[F(t)]} \ , \ k = 1, 2, 3, 4$$

Note that the first element $H_1^{\text{exp}}(f)$ represents the co-located FRF. The corresponding plots are represented in magnitude and phase as follows:

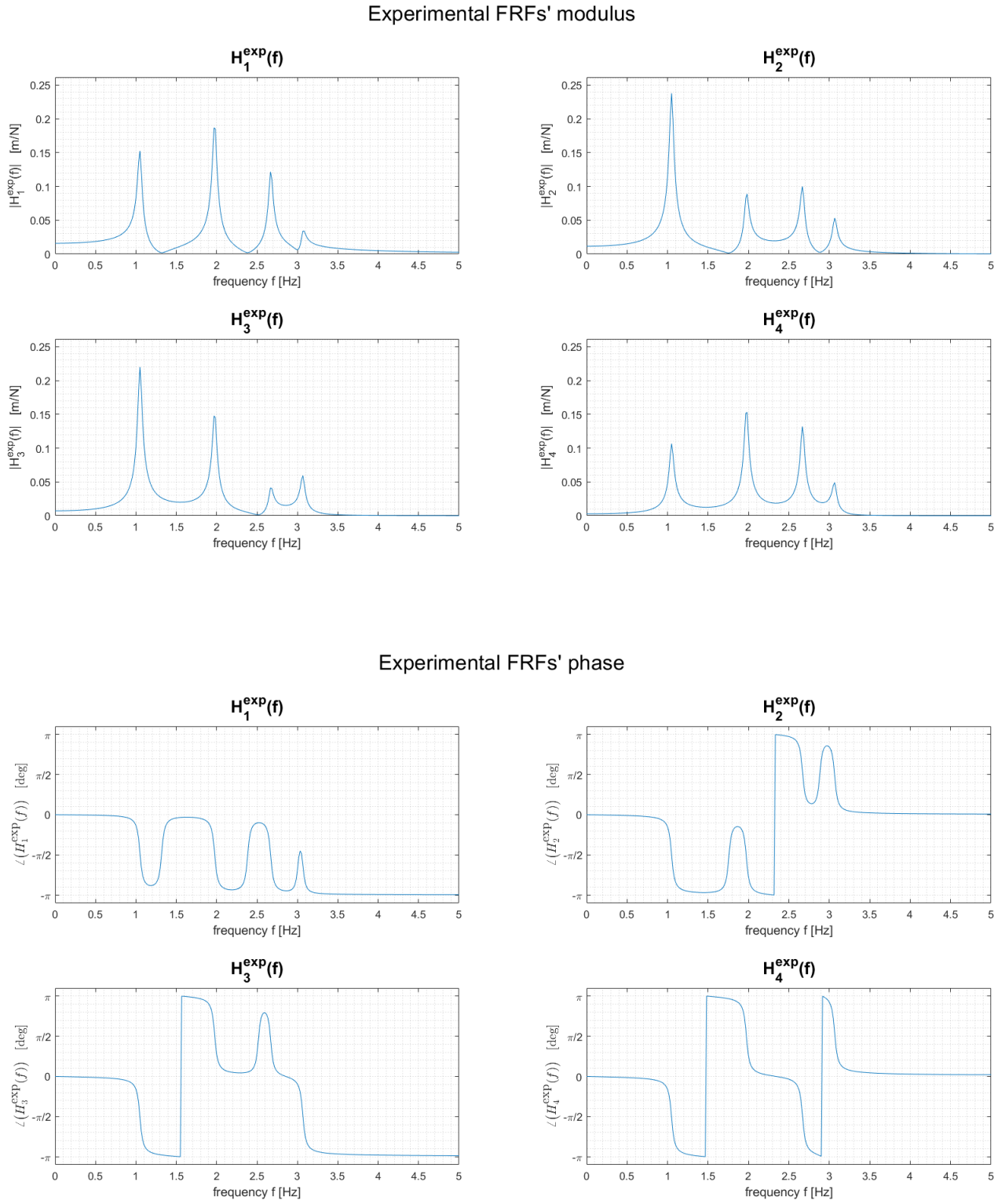

2 Simplified methods for model identification

To estimate the system parameters, we first reached for simplified methods. The assumption we are working under are, as usual, low damping (order of magnitude for ξ: $10{-}2$), and well-distincted peaks in amplitude spectrum. As long as the damped frequencies are concerned, we found the relative maxima in each FRF setting one order of magnitude lower than the absolute maximum as threshold, and then found the frequencies corresponding to those values. The resulting matrix of damped frequencies is:

$$\mathbf{f_d} = \begin{bmatrix} f_{\mathrm{d}_1}^{(1)} & f_{\mathrm{d}_1}^{(2)} & f_{\mathrm{d}_1}^{(3)} & f_{\mathrm{d}_1}^{(4)} \\ f_{\mathrm{d}_2}^{(1)} & f_{\mathrm{d}_2}^{(2)} & f_{\mathrm{d}_2}^{(3)} & f_{\mathrm{d}_2}^{(4)} \\ f_{\mathrm{d}_3}^{(1)} & f_{\mathrm{d}_3}^{(2)} & f_{\mathrm{d}_3}^{(3)} & f_{\mathrm{d}_3}^{(4)} \\ f_{\mathrm{d}_4}^{(1)} & f_{\mathrm{d}_4}^{(2)} & f_{\mathrm{d}_4}^{(3)} & f_{\mathrm{d}_4}^{(4)} \end{bmatrix} = \begin{bmatrix} 1.0500 & 1.9667 & 2.6667 & 3.0833 \\ 1.0500 & 1.9833 & 2.6667 & 3.0667 \\ 1.0500 & 1.9667 & 2.6667 & 3.0667 \\ 1.0500 & 1.9833 & 2.6667 & 3.0667 \end{bmatrix}$$

where every row corresponds to one of the four different measurements, and each column to a vibration mode. The values are affected by small fluctuations as for the 2^{nd} and 4^{th} frequency, so we can reckon the values overall agree with each other. In order to have one value for each mode, we averaged the values for the four measurements and for each of the modes, obtaining

$$\mathbf{f_d} = \begin{bmatrix} 1.05 & 1.97 & 2.67 & 3.07 \end{bmatrix}$$

As a second step, we searched for the adimensional damping ratios, applying the half-power bandwidth method. This exploits the relationship between the width of a resonating mode bell-like peak and the damping ratio, which are dirctly proportional. Each ratio for each measurement is computed thanks to the formula

$$\xi_i = \frac{(f_2^{(i)})^2 - (f_1^{(i)})^2}{4\,(f_{\mathrm{d}}^{(i)})^2}\ ,\ i = 1, 2, 3, 4$$

i being the mode number. The resulting matrix of damping ratios is:

$$\boldsymbol{\xi} = \begin{bmatrix} \xi_1^{(1)} & \xi_1^{(2)} & \xi_1^{(3)} & \xi_1^{(4)} \\ \xi_2^{(1)} & \xi_2^{(2)} & \xi_2^{(3)} & \xi_2^{(4)} \\ \xi_3^{(1)} & \xi_3^{(2)} & \xi_3^{(3)} & \xi_3^{(4)} \\ \xi_4^{(1)} & \xi_4^{(2)} & \xi_4^{(3)} & \xi_4^{(4)} \end{bmatrix} = \begin{bmatrix} 0.0159 & 0.0128 & 0.0062 & 0.0081 \\ 0.0159 & 0.0084 & 0.0062 & 0.0054 \\ 0.0159 & 0.0128 & 0.0094 & 0.0054 \\ 0.0159 & 0.0126 & 0.0062 & 0.0081 \end{bmatrix}$$

organized like the damped frequency matrix. This time, the values vary a little more than before: this is due to non-negligible variations of the peaks width relative to the same resonance in distinct measurements, especially for mode 2 in measurement 2 and mode 3 in measurement 3. As for the 4^{th} mode, conformity between measurement 1 and 4 and between measurement 2 and 3 may be observed. Values for the 1^{st} mode are the most accurate both for the frequency value and for the damping ratio, in accordance to the fact the more the resonances are clear and their peaks are sharp for each measurement, the easier it is to make an estimation, because values will tend to be the same for all of the measurements. In fact, the first mode corresponds to a very clear peak for each of them. Analogously to what we did for the natural frequencies, we arrived to a single value of ξ for each mode computing the mean among the measurements. This time, though, we excluded values that more clearly differ from the others: the one for mode 2 and measurement 2 and the one for mode 3 and measurement 3. The final values are then

$$\boldsymbol{\xi} = \begin{bmatrix} 0.0159 & 0.0127 & 0.0062 & 0.0068 \end{bmatrix}$$

Finally, the mode shape of i-th mode is estimated equalling the experimental FRF for measurement $k = 1, 2, 3, 4$, computed in the previous section and evaluated at the i-th resonance frequency, $i = 1, 2, 3, 4$, to the approximated FRF $H_k^{\mathrm{approx}^{(i)}}$ connecting displacement of point k and the force, evaluated at the resonant frequencies. The mode shape element relative to the force application position has been neglected, being it the same for all of the FRFs.

$$
\begin{aligned}
&H_k^{\exp}(\omega_{\mathrm{d}_k}^{(i)}) \approx H_k^{\mathrm{approx}^{(i)}}(\omega_{\mathrm{d}_k}^{(i)}) = \frac{\phi_k^{(i)}}{-\omega^2 m_k^{(i)} + j\omega c_k^{(i)} + k_k^{(i)}}\Big|_{\omega=\omega_{\mathrm{d}_k}^{(i)}} = \frac{\phi_k^{(i)}}{j\omega_{\mathrm{d}_k}^{(i)} c_k^{(i)}} = -j\frac{\phi_k^{(i)}}{\omega_{\mathrm{d}_k}^{(i)} c_k^{(i)}} \\
&\Rightarrow\ j\frac{\phi_k^{(i)}}{\omega_{\mathrm{d}_k}^{(i)} c_k^{(i)}} \approx -H_k^{\exp}(\omega_{\mathrm{d}_k}^{(i)})\ \Rightarrow\ \frac{\phi_k^{(i)}}{\omega_{\mathrm{d}_k}^{(i)} c_k^{(i)}} \approx \Im\{-H_k^{\exp}(\omega_{\mathrm{d}_k}^{(i)})\} = -\Im\{H_k^{\exp}(\omega_{\mathrm{d}_k}^{(i)})\} \\
&\Rightarrow\ \phi_k^{(i)} \approx -\Im\{H_k^{\exp}(\omega_{\mathrm{d}_k}^{(i)})\}\,\omega_{\mathrm{d}_k}^{(i)} c_k^{(i)}\ ,\ i,k = 1,2,3,4
\end{aligned}
\tag{1}
$$

where the contributions of other modes other than the i-th mode have been neglected in the computation of the i-th mode shape. The damping coefficients $c_k^{(i)}$ have been derived from the damping ratios following the definition of damping ratio:

$$
\xi_k^{(i)} = \frac{c_k^{(i)}}{2\, m_k^{(i)} \omega_{\mathrm{d}_k}^{(i)}}\ \Rightarrow\ c_k^{(i)} = 2\,\xi_k^{(i)} m_k^{(i)} \omega_{\mathrm{d}_k}^{(i)}
$$

and setting the elements of the modal mass matrix $m_k^{(i)}$ to 1. The modal matrix of all the elements $\phi_k^{(i)}$ is reported here:

$$
\boldsymbol{\phi} = \begin{bmatrix} \phi_1^{(1)} & \phi_1^{(2)} & \phi_1^{(3)} & \phi_1^{(4)} \\ \phi_2^{(1)} & \phi_2^{(2)} & \phi_2^{(3)} & \phi_2^{(4)} \\ \phi_3^{(1)} & \phi_3^{(2)} & \phi_3^{(3)} & \phi_3^{(4)} \\ \phi_4^{(1)} & \phi_4^{(2)} & \phi_4^{(3)} & \phi_4^{(4)} \end{bmatrix} = \begin{bmatrix} 0.1050 & 0.3438 & 0.2130 & 0.0683 \\ 0.1642 & 0.1065 & -0.1725 & -0.1071 \\ 0.1519 & -0.2704 & -0.1083 & 0.1195 \\ 0.0735 & -0.2841 & 0.2303 & -0.1465 \end{bmatrix}
$$

Normalizing the elements of each measure taking the first one as reference the result is

$$
\boldsymbol{\phi} = \begin{bmatrix} 1 & 1 & 1 & 1 \\ 1.5632 & 0.3098 & -0.8098 & -1.5669 \\ 1.4459 & -0.7867 & -0.5087 & 1.7482 \\ 0.7000 & -0.8264 & 1.0811 & -2.1442 \end{bmatrix}
$$

These values are in agreement with the magnitude and phase plots of 1: the modulus of $\phi_k^{(i)}$ is approximatedly the relative value in the amplitude plots, while its sign follows the sign of the phase in the phase plots. The biggest divergence between the absolute value of the elements in the modal matrix and the plotted values is about measurement 3, 3$^{\mathrm{rd}}$ mode, which should have a relative magnitude of $\frac{1}{3}$ with respect to the 1$^{\mathrm{st}}$ measurement, but the corresponding element in $\boldsymbol{\phi}$ indicates $\frac{1}{2}$. This is certainly due to the approximated values of the modal matrix, obtained by means of a simplified method. In the next section, we go on with the analysis using a more accurate procedure, which is a modal parameter identification model.

3 Modal parameter identification

Modal identification uses the modal approach as analytical support, meaning that it reconstructs the analytical transfer function $H_k(\omega)$ of the system considering it as if it were made up of many one-DOF systems, since the various degrees of freedom are defined by the modal variables. $H_k(\omega)$ represents the harmonic transfer function for an output at the generic point k (recall that the input position is fixed) of the N-DOF system considered. So this transfer function will have modal parameters as unknown quantities:

$$H_k(\omega) = H_k(\omega, \omega_{\mathrm{d}_k}^{(i)}, m_k^{(i)}, k_k^{(i)}, \xi_k^{(i)}, \phi^{(i)}) \ , \ i, k = 1, 2, 3, 4$$

being:

- ω_{d_k} the natural frequencies;
- $m_k^{(i)}$ the modal masses;
- $k_k^{(i)}$ the modal stifness;
- $\xi_k^{(i)}$ the damping ratio;
- $\phi_k^{(i)}$ the element of the modal matrix $\boldsymbol{\phi}$.

With this approach, the dynamic response of the structure subjected to the known excitation is measured at several k points; this dynamic response, expressed in terms of experimental transfer functions $H_k^{\exp}(\omega)$, is then compared to the analytical response $H_k^{\mathrm{num}}(\omega)$ defined beforehand by minimising the difference between the analytical values and the experimental ones. It is thus possible to determine the set of modal parameters needed to characterize the static and dynamic behaviour of the system being analyzed.

From the modal approach theory, we know that, as far as a sufficient number of modes N are considered, the following gives the expression for $H_k^{\exp}(\omega)$:

$$H_k^{\exp}(\omega) = \sum_{i=1}^{N} \frac{\phi_k^{(i)}}{-\omega^2 m_k^{(i)} + j\omega c_k^{(i)} + k_k^{(i)}} \ , \ i, k = 1, 2, 3, 4$$

where, like in equation (1), k is the measurement index, and the element of the modal matrix relative to the forcing position has been neglected.

For well distinguished peaks and lightly damped structures, the experimental Frequency Response Function $H_k^{\exp}(\omega)$ can be approximated by the analytical Frequency Response Function $H_k^{\mathrm{num}}(\omega)$ around a certain $\omega_{\mathrm{d}_k}^{(i)}$ as:

$$H_k^{\mathrm{num}}(\omega) = \frac{A_k^{(i)} + jB_k^{(i)}}{-\omega^2 m_k^{(i)} + j\omega c_k^{(i)} + k_k^{(i)}} + C_k^{(i)} + jD_k^{(i)} + \frac{E_k^{(i)} + jF_k^{(i)}}{\omega^2}$$

In this form:

- the first term represent the contribution of the **resonating mode** in our frequency range of interest;
- the second term represent the contribution of the modes at **higher** frequency than $\omega_{\mathrm{d}_k}^{(i)}$; this contribution is approximately constant because our frequency range of interest falls in the **quasi-static region** of these modes;
- the third term represents the contribution of the modes at **lower** frequency than $\omega_{\mathrm{d}_k}^{(i)}$; this contribution has approximately a $\frac{1}{\omega^2}$ behavior because our frequency range of interest falls in the **seismographic region** of these modes.

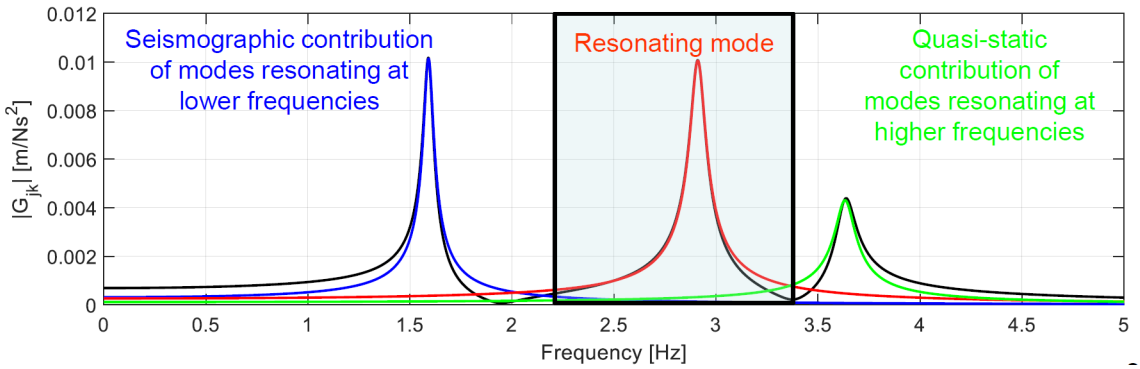

The frequency ranges of interest are partitions of the frequency axis. Given the N well distinguished peaks, we will have N ranges of interest. We chose to compute the bounds of these ranges as the local minima between one peak and the following one. The following depicts the minima and maxima we considered.

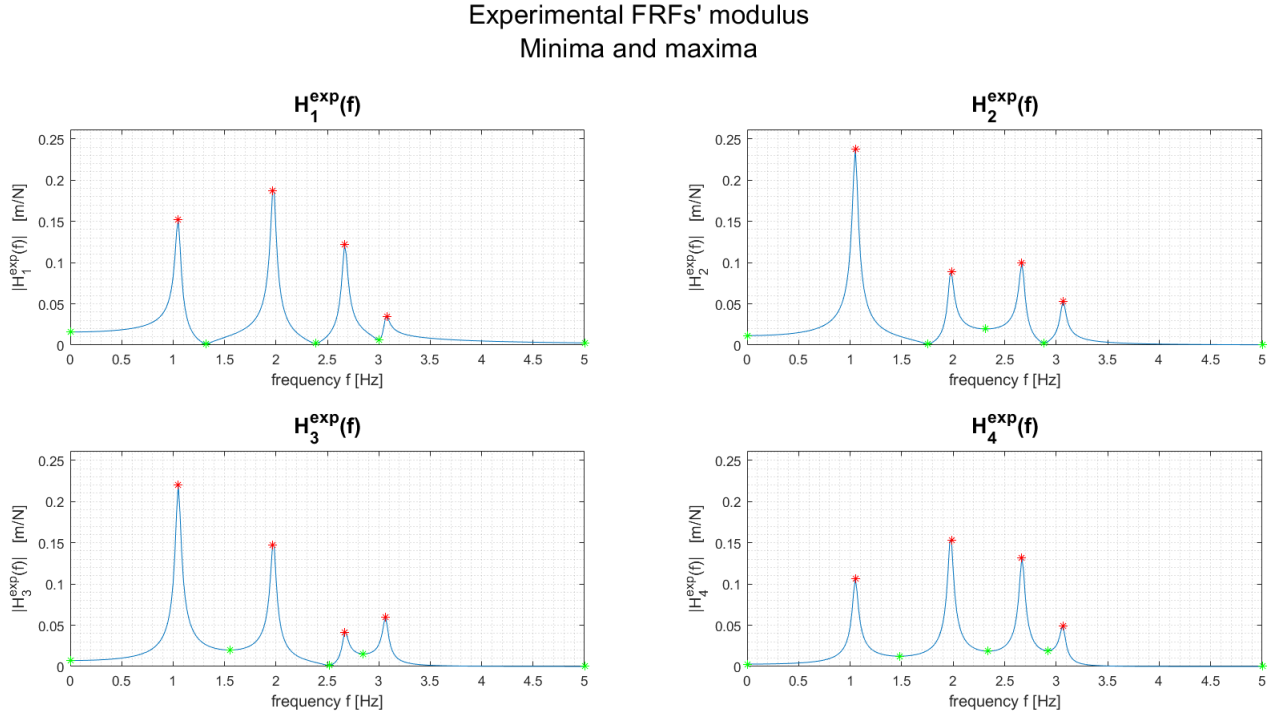

3.a Vibration modes identification procedure

For a given set of experimental FRFs $H_k^{\exp}(\omega)$, obtained for a fixed excitation location and different measurement locations k (4 points), a least squares minimization procedure can be implemented for the estimation of the modal parameters.

The error function to be minimized (cost function) is:

$$\varepsilon = \sum_{s=s_{\inf}}^{s_{\sup}} \Re^2\{H_k^{\exp}(\omega_s) - H_k^{\text{num}}(\omega_s)\} + \Im^2\{H_k^{\exp}(\omega_s) - H_k^{\text{num}}(\omega_s)\}$$

Since the error function depends non-linearly on the unknown parameters, an iterative minimization procedure is used. This is implemented in MATLAB throught the function `fminsearch`. According to the documentation, `fminsearch` is a nonlinear programming solver. It searches for the minimum of a problem specified by $\min_x f(x)$. Its syntax is: `x = fminsearch(fun, x0, options)`.

`fun` is the function to minimize, specified as a function handle or function name. `fun` is a function that accepts a vector or array `x` and returns a real scalar `f` (the objective function evaluated at `x`).

An initial guess vector `x0` (`xpar0` in our code) is required, consisting of a preliminary estimate of:

1. $\omega_{\mathrm{d}_k}^{(i)}$ which is found from the maximum peak in the considered frequency range. We already discussed the procedure in section 2. It has been evaluated from each FRF and then averaged.

2. $\xi_k^{(i)}$ which is found through a simplified method (in our case the half power bandwidth method). We already discussed the procedure in section 2. It has been evaluated from each FRF and then averaged.

3. $A_k^{(i)}$ which is found considering each FRF at resonance and assuming real valued mode shapes (valid in resonance condition):

$$\phi_k^{(i)} = -\Im\{H_k^{\exp}(\omega_{\mathrm{d}_k}^{(i)})\}\,\omega_{\mathrm{d}_k}^{(i)} c_k^{(i)} = A_k^{(i)}$$

   Again, we already discussed the procedure in section 2. It follows that $B_k^{(i)} = 0$.

4. $C_k^{(i)}, D_k^{(i)}, E_k^{(i)}, F_k^{(i)}$ are set to zero under the assumption of sufficiently distinguished peaks.

The non-linear minimization procedure elaborates separately the FRFs, leading to an estimate of the modal parameters $\omega_{\mathrm{d}_k}^{(i)}, \xi_k^{(i)}, A_k^{(i)}$ for every frequency range (i.e. for every peak) and for every measurement. Then the parameters are averaged. A further improvement of the algorithm could be to perform the minimization simultaneously on the whole set of FRFs, leading to a more precise estimate of the modal parameters. In this case the information given by the correlation of the FRFs is exploited. The quality of the estimates can be visually assessed comparing in a plot the identified FRFs $H_k^{\mathrm{num}}(\omega)$ with the experimental ones $H_k^{\exp}(\omega)$: as for the moduli, we may conclude the algorithm worked very well for the 2^{nd}, 3^{rd} and 4^{th} mode, being the curves we started with very well approximated by the results, and fairly well for the 1^{st} mode, for which the quasi-static contributions of the other modes, which we neglected for the initial guess of the minimization, could be playing a greater role than for the other modes. Nevertheless, the most relevant reason for the lack in precision is the fact the frequency ranges taken into account are too tight, meaning that the first mode actually would go a bit beyond the bound we set in frequency. The phase plots show an overall quite good reconstruction, with just a couple of plots showing other $-90°$ jumps after the correct one.

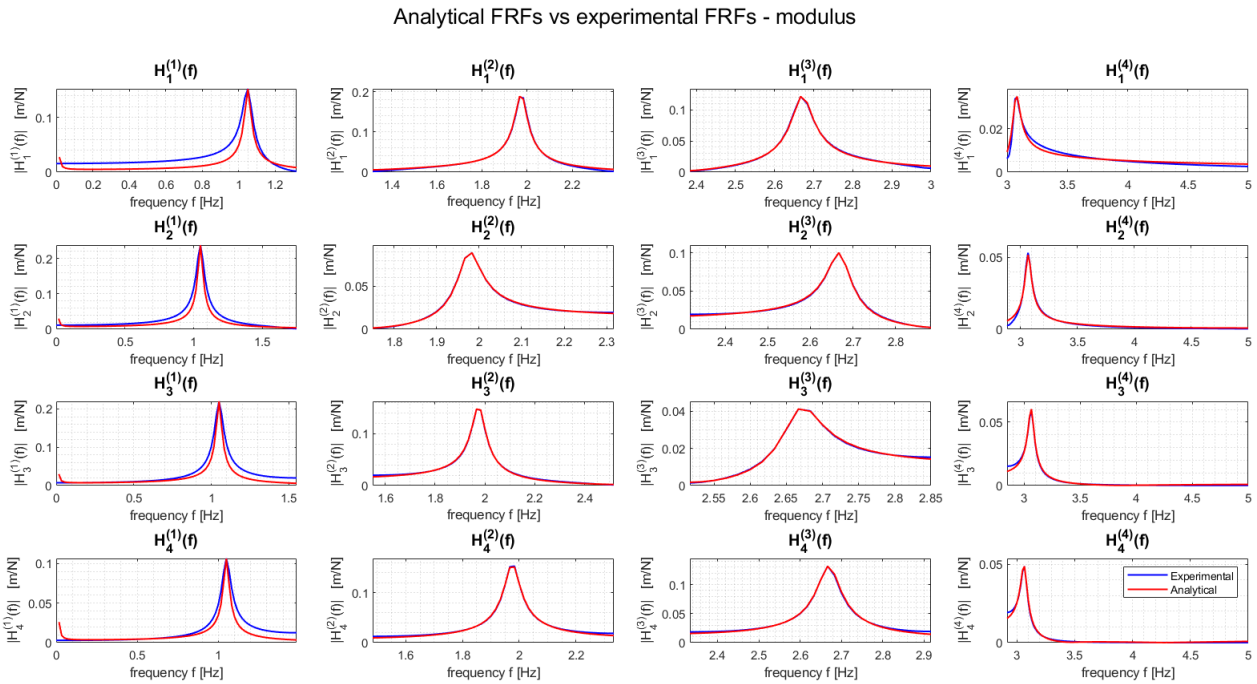

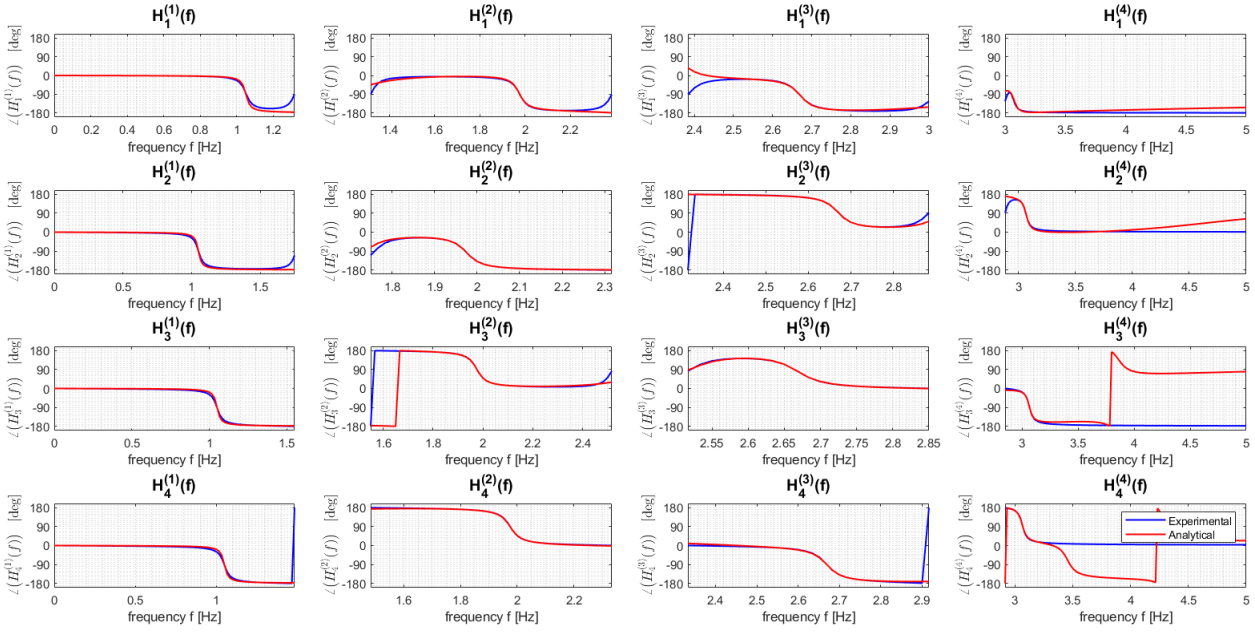

4 Modal parameter comparison

The estimated modal parameters have been reduced to a single value per mode as for the simplified methods of section 2, averaging among the measurements and resulting in the following vectors:

$$\mathbf{f_d} = \begin{bmatrix} 1.050 & 1.975 & 2.669 & 3.068 \end{bmatrix} \quad , \quad \boldsymbol{\xi} = \begin{bmatrix} 0.0159 & 0.0136 & 0.0100 & 0.0092 \end{bmatrix}$$

Instead, the normalized modal matrix is

$$\phi = \begin{bmatrix} 1 & 1 & 1 & 1 \\ 1.5632 & 0.4579 & -0.8252 & -1.4745 \\ 1.4459 & -0.8050 & -0.3504 & 1.7016 \\ 0.7000 & -0.8510 & 1.1423 & -1.5256 \end{bmatrix}$$

All the results are very similar to those obtained with the simplified approach. The greatest divergences are found in the modal matrix, which now should be more accurate.

5 FRFs reconstruction